RESEARCH MEMORANDUM

PERFORMANCE OF TWO AIR-COOLED TURBOJET ENGINES DETERMINED ANALYTICALLY FROM ENGINE COMPONENT PERFORMANCE FOR A RANGE OF COOLING-AIR WEIGHT FLOWS

By Robert R. Ziemer, Louis J. Schafer, Jr., and Thomas R. Heaton

Lewis Flight Propulsion Laboratory
Cleveland, Ohio

NATIONAL ADVISORY COMMITTEE
FOR AERONAUTICS

WASHINGTON

February 18, 1954

NATIONAL ADVISORY COMMITTEE FOR AERONAUTICS

RESEARCH MEMORANDUM

PERFORMANCE OF TWO AIR-COOLED TURBOJET ENGINES DETERMINED ANALYTICALLY FROM ENGINE COMPONENT PERFORMANCE FOR A RANGE OF COOLING-AIR WEIGHT FLOWS

By Robert R. Ziemer, Louis J. Schafer, Jr., and Thomas R. Heaton

SUMMARY

In an analysis of two turbojet engines, the component performance of the compressors and turbines was used to determine the effect on engine performance and operation of bleeding the compressor to furnish cooling air for the turbine rotor blades. The engines considered were a centrifugal-flow-compressor engine of 4000 pounds thrust and an axial-flow-compressor engine of approximately 6000 pounds thrust.

The results indicated an increase of approximately 2.0 percent in thrust specific fuel consumption for every 0.01 increase in required cooling-air-flow ratio for both engines when operated at rated speed and constant thrust conditions.

By the use of air-cooled turbine rotor blades, which permit operation at higher turbine-inlet temperatures, increases in specific thrust (up to 24 percent) could be obtained for both engines. Accompanying the increase in specific thrust was an increase in thrust specific fuel consumption of 4.9 percent for the centrifugal-flow engine and about $17\frac{1}{2}$ percent for the axial-flow machine. The magnitude and the differences in the increase of thrust specific fuel consumption are applicable, within the limitations imposed by the method of analysis used, only to the two engines considered. For these specific engines, the differences in the increase of thrust specific fuel consumption were due primarily to the lower cooling effectiveness of the air-cooled turbine blades used in the axial-flow engine and the increase in turbine efficiency of the centrifugal-flow engine.

Because of the change in the compressor and turbine operating points with varying amounts of cooling-air, the effect of cooling should be considered in the engine design in order to realize the highest possible component efficiencies.

INTRODUCTION

As part of the turbine-cooling program at the NACA Lewis laboratory, an analysis was made of two turbojet engines at sea-level static conditions, the engine component characteristics being used to determine the magnitude and the causes of changes in engine performance when the turbine rotor blades are cooled with air bled from the compressor exit. The experiments of references 1 to 4 and the analysis of reference 5 indicate that satisfactory operation can be expected from air-cooled turbine blades made from noncritical materials at cooling-air to compressor-inlet-air-flow ratios of 0.03 or below at present-day turbine-inlet temperatures. The experimental investigations reported in references 6 and 7 and the analysis of reference 8 show that the design of disks to support the air-cooled blades and to duct the cooling air to them represent no radical changes in the concept of turbine disk design. Therefore, the use of air-cooled turbines appears feasible either to permit the use of noncritical materials in the construction of the turbine, or to capitalize on the available gains of operation at increased turbine-inlet temperatures.

Preliminary analysis of the effect of air-cooling a particular turbine on engine performance is presented in reference 9, where, for a specified turbine-inlet temperature and the required cooling-air-flow ratio for a particular air-cooled turbine blade, the specific thrust decreased relative to the zero coolant-flow condition, and the specific fuel consumption increased. The analysis of reference 9, where no consideration was given to changes in the turbine and compressor operating characteristics as various amounts of air were bled for cooling, is adequate if the turbine aerodynamics are changed to meet a specific design-point condition. However, for off-design operation or applying cooling to an existing turbine with no changes in turbine blade geometry, the compressor and turbine operational characteristics must be known in order to obtain a realistic evaluation of the effect of cooling on engine performance. For this latter case, the analysis presented herein was conducted.

Two turbojet engines were considered - a centrifugal-flow-compressor engine of 4000 pounds thrust and a 12-stage axial-flow-compressor engine of approximately 6000 pounds thrust. In this analysis, the performance was evaluated for both engines at sea-level static conditions by matching the operational characteristics of their compressors and single-stage highly loaded air-cooled turbines over a range of cooling-air-flow ratios, jet nozzle areas, and engine speeds. The operational points of the engines with the cooling requirements of specific air-cooled turbine rotor blades were also determined. The cooling air for the turbine blades was assumed to be bled from the compressor exit and discharged into the main gas stream.

For the centrifugal-compressor engine, a turbine blade having a cooling effectiveness equal to that of configuration B, profile 1, of reference 5 was used. An air-cooled blade similar to configuration H, profile 2, of reference 5 was used for the axial-flow-compressor engine. Reference 10 presents the performance in cold air for a scale model of the turbine considered herein for the axial-flow-compressor engine. This turbine was designed as an air-cooled substitution for the production turbine; the rotor has 72 nontwisted blades of uniform camber. The results of reference 10 were used to predict the turbine performance in the full-scale engine. For the centrifugal-compressor engine, unpublished results of a cold-air performance investigation similar to that of reference 10 were utilized. The turbine configuration was identical to that of the actual production engine, and it was assumed that cooling could be incorporated in the turbine rotor blades without altering their aerodynamic performance.

The results of the present analysis indicate the effects of bleeding various amounts of cooling air from the compressor exit on the turbine and compressor operating points, turbine-inlet temperature, engine specific thrust, and engine thrust specific fuel consumption. Also presented are the specific thrust, specific fuel consumption, and turbine-inlet temperature under which each engine could operate with a specific air-cooled turbine rotor blade at a constant blade temperature. Consideration is given to the effect on engine performance of using part of the cooling air bled from the compressor to cool the turbine stator blades and part to cool the rotor blades.

ANALYSIS AND CALCULATION PROCEDURE

Compressor and Turbine Matching

The analysis of this report was made by matching the turbine and compressor performance when various cooling-air weight flows were bled from the engine compressor exit. The turbine performance characteristics were obtained from cold-air tests on scale models, and the compressor performance from maps obtained on full-scale compressors. For the centrifugal-compressor-engine calculations, the map of the standard free-vortex uncooled turbine was used, with the assumption that the cooled turbine of this report would have the same aerodynamic performance. The axial-compressor-engine calculations were made with the performance map of a cooled turbine having nontwisted rotor blades and twisted stator blades. This turbine was designed by the NACA, and its performance characteristics are reported in reference 10.

The matching of the compressor and turbine components of the engines was accomplished by related parameters of these components (see ref. 11). The following assumptions were made in the matching calculations and in the determination of the engine performance:

(1) The turbine work equals the work required to drive the compressor plus the work to pump the cooling air from the entrance of the turbine rotor to the tips of the rotor blades. Power required by auxiliaries, bearings, and disk windage is thus zero.

(2) The pressure loss in the bleed piping is zero.

(3) The gas temperature profile at the turbine inlet is uniform in both circumferential and spanwise directions.

(4) The heat loss from the engine to the surrounding air is zero.

(5) The mixing of the cooling air from the blade tips with the combustion gases occurs with no loss in total pressure.

(6) The effect of the discharge of the cooling air from the tips of the rotor blades on turbine performance is negligible.

(7) The jet nozzle efficiency is equal to 1.0.

Several factors in the analysis used herein might cause differences between the theoretical engine performance obtained with the cold-air turbine maps and the actual engine performance: (1) the magnitude of the effects of the cooling-air discharging from the blade tips in the engine installation, (2) the nonuniform turbine-inlet-gas temperature profile that exists in the engine, and (3) the Reynolds number effect resulting when the cold-air tests are made on a small-scale model of the actual turbine. It is expected, however, that, although the magnitude of values of thrust, specific fuel consumption, and efficiencies obtained from calculations as outlined herein may be in error, the trends obtained should be representative.

The general procedure followed in making the turbine and compressor matching calculations was to assume an operating point on the compressor map along a particular corrected compressor speed line. Next, the turbine conditions that would permit the turbine to pass the mass flow and deliver the required work for the correct equivalent tip speed were determined. The resulting jet nozzle area, consistent with the pressure and temperature conditions downstream of the turbine, was then determined; and the engine thrust and fuel consumption were calculated. This was done over a range of compressor operating points for each of four arbitrarily selected cooling-air-flow ratios (0, 0.02, 0.04, and 0.06). The calculated engine, compressor, and turbine performance parameters, such as engine temperature ratio, specific thrust, thrust specific fuel consumption, and so forth, were plotted against the calculated jet nozzle areas for the four arbitrarily selected cooling-air-flow ratios at the engine speeds considered. The values of engine, compressor, and turbine performance parameters at constant jet nozzle areas could then be read from these plots.

A detailed description of the calculation procedure for the compressor and turbine matching and the engine and turbine performance for various cooling-air-flow ratios is presented in appendix B. The engine calculation stations are shown in figure 1, and symbols are listed in appendix A.

Corrugated-Insert-Blade Cooling-Air Requirements

The engine operating conditions were determined for a specific corrugated-insert air-cooled turbine rotor blade operating at cooling-air-flow ratios to maintain stress safety factors of 2.0 and 3.0. The information on the blade cooling performance needed to determine the curves was obtained from reference 5. The blade configurations considered in this report are designated in reference 5 as profile 1, configuration B, for the engine using the centrifugal-flow compressor and profile 2, configuration H, for the engine using the axial-flow compressor (see fig. 2). The air-cooled blades considered herein were convection-cooled blades with the cooling air entering the blade through the root section. The center of the hollow shell was blocked by an insert that forced the cooling air to flow in an annulus next to the blade shell. The annulus was packed with a corrugated sheet that contacted both the insert and the shell and increased the heat-transfer-surface area.

With the information presented in reference 5, it was possible to plot the temperature-difference ratio $\varphi = \frac{\overline{T}_{g,e} - \overline{T}_B}{\overline{T}_{g,e} - \overline{T}_{a,e,h}}$ against the cooling-air-flow ratio w_a/w_1 for a specific value of $\overline{T}_{g,e}$ and $\overline{T}_{a,e,h}$. The following equation was derived from an approximation of the linear radial blade temperature-distribution equation (eq. (1) of ref. 5):

$$\varphi = \frac{1}{1 + K_2 \left\{ \frac{\left[w_3 (\overline{T}_{g,e}/\overline{T}_B) \right]^{0.7}}{\left[w_a (\overline{T}_{a,e,h}/T_B) \right]^{0.8}} \right\}} \qquad (1)$$

In deriving this equation from the equation of reference 5, the outside blade heat-transfer coefficient was evaluated in terms of the product of the combustion-gas weight flow and the ratio of combustion-gas to blade-wall temperature raised to the 0.7 power. The inside blade surface heat-transfer coefficient was evaluated in terms of the product of the cooling-air weight flow and the ratio of cooling-air to blade-wall temperature raised to the 0.8 power. The results of the exact equation of reference 5 were then used to evaluate the constant K_2 in equation (1) of this report. Then, for a given value of w_3, a curve was plotted of the temperature-difference ratio φ against cooling-air-flow ratio for several effective gas temperatures and a specific effective

cooling-air inlet temperature. A second curve could then be plotted of the effective gas temperature against the turbine rotor blade temperature for different constant cooling-air-flow ratios.

Engine operating lines with the turbine blades operating at two values of average blade temperature were investigated. The average blade temperatures were evaluated from a consideration of blade safety factors of 2.0 and 3.0. The safety factor is defined as the ratio of the allowable stress determined from 100-hour stress-rupture data (or 0.2-percent yield data, as applicable) for the blade material (Timken 17-22A(S)) to the actual centrifugal stress at the critical section of the blade. (The blade material creep rate was not considered.) The critical section was located approximately 1.5 inches from the root for the blades considered in this analysis. The blade stress corresponding to these safety factors was determined by multiplying the actual centrifugal blade stress at the critical section by the safety factor. From this resulting blade stress and the curve of temperature against material stress-rupture, the allowable blade-wall temperature for the particular safety factor could be obtained.

When the allowable blade temperature was obtained, the effective gas temperature at various cooling-air-flow ratios could be read from the previously determined curve of $\overline{T}_{g,e}$ against $\overline{T}_B$. The allowable turbine-inlet temperature (and thus engine temperature ratio) could be evaluated from the allowable effective gas temperature $\overline{T}_{g,e}$ when the stator discharge angle, the turbine rotor speed, and the stator discharge Mach number were known.

RESULTS AND DISCUSSION

Compressor and Turbine Performance Characteristics

Figure 3 shows the variation of corrected compressor-inlet weight flow with corrected engine speed for the range of cooling-air-flow ratios and a fixed jet nozzle area. The values of jet nozzle area are those for rated thrust at zero cooling-air-flow ratio. For a fixed engine speed and jet nozzle area, the effect of bleeding air at the compressor discharge for cooling the turbine rotor blades on compressor weight flow was slightly greater for the centrifugal-compressor engine (fig. 3(a)) than for the axial-flow-compressor engine (fig. 3(b)) because of the peculiar characteristics of the two types of compressors. The change in the operating point on the compressor map at a given jet nozzle area and compressor speed for the centrifugal compressor was reflected primarily in the compressor weight-flow change, while the compressor pressure ratio remained essentially constant. For the axial-flow compressor, the reverse was true: The compressor-inlet weight flow was almost constant;

and the change in compressor operating point, due to bleed at a particular jet nozzle area and compressor speed, was to higher compressor pressure ratios as the amount of discharge bleed was increased.

Figures 4 and 5 present the variation of engine temperature ratio and turbine pressure ratio, respectively, with corrected engine speed for the two engines when the compressor and turbine are matched for a constant jet nozzle area and various cooling-air-flow ratios. For each increase of 0.01 in cooling-air-flow ratio at rated engine speed, the turbine-inlet temperature increased approximately 60° F for both the centrifugal- and the axial-compressor engines (fig. 4). Decreases of 0.02 and 0.025 in turbine pressure ratio for each 0.01 increase in cooling-air-flow ratio were obtained for the centrifugal- and the axial-compressor engines, respectively (fig. 5). This small decrease in turbine pressure ratio was a result of turbine operation at higher turbine-inlet temperature levels.

The range of operation of the centrifugal compressor for the cooling-air-flow ratios considered is shown in figure 6(a), where operating lines for cooling-air-flow ratios of 0 and 0.06 are drawn on the compressor map. The map is presented on a relative basis, with the engine design point (zero cooling-air flow at rated engine speed at a jet nozzle area of 1.80 sq ft) designated as 1.0. At the rated-engine-speed condition, the compressor weight flow at a cooling-air-flow ratio of 0.06 was 2.0 percent less than that at zero cooling-air-flow ratio. This shift in the engine operating line resulted in an increase in compressor efficiency of about 1.0 percent and also moved the compressor operation closer to the surge line.

The decrease in compressor weight flow at a fixed jet nozzle area is caused by an increase in turbine-inlet temperature when air is bled for cooling, which, in turn, is effected by two conditions: When the compressor is bled, so that less air is flowing through the turbine, the specific turbine work must increase; and a further increase in specific turbine work is brought about by the work required to accelerate the cooling air (bled from the compressor) to the turbine tip speed. This increase is accomplished by an increase in turbine-inlet temperature; and, since the turbine stator blades are choked and the compressor-exit pressure is essentially constant, the turbine, and consequently the compressor, weight flow must decrease.

The engine operating lines of the centrifugal-compressor engine for cooling-air-flow ratios of 0, 0.02, 0.04, and 0.06 are shown on the turbine map in figure 6(b). This map is presented on a relative basis with the design point taken as the reference point and assigned the value of 1.0. At the rated-engine-speed condition, the relative corrected specific turbine work $(\Delta h_T'/\theta_3^*)_R$ decreases about 5 percent as the cooling-air-flow ratio is increased from 0 to 0.06 at a constant jet nozzle area.

(The relative corrected specific turbine work is defined as the ratio of the corrected specific turbine work at any operating condition to the corrected specific turbine work at the design condition.) This decrease in corrected specific turbine work is due primarily to operation at a higher turbine-inlet temperature. This shift of the engine operating point with cooling-air-flow ratio is accompanied by an increase of 1 point in the turbine efficiency at the rated-speed condition. At a relative engine speed of 0.870, the shift of the engine operating point with increasing cooling-air-flow ratio results in a decrease in the turbine efficiency of about $1\frac{1}{2}$ points. The change in engine operating point with an increase in cooling-air-flow ratio from 0 to 0.06 to a point of lower corrected tip speed and lower corrected specific turbine work is accompanied by a decrease in turbine pressure ratio of approximately 4 percent.

3021

The axial-flow-compressor map in figure 7(a) shows operating lines for zero cooling-air flow and a cooling-air-flow ratio of 0.06 for a constant jet nozzle area. Because of the characteristics of an axial-flow compressor, the compressor weight flow did not change appreciably when the cooling-air was bled, but the compressor pressure ratio increased 3 percent with a cooling-air-flow ratio of 0.06 at the rated-speed condition. The compressor efficiency also increased with the bleeding of cooling air from the compressor. However, because the shift of the engine operating line was so slight, the change in the compressor efficiency was only about 1/2 point. Bleeding cooling air from either the centrifugal- or the axial-flow compressor moves the compressor operating point in the direction of compressor surge. Whether or not this is a serious consideration depends on the particular engine design. For the two cases considered in this report, the centrifugal compressor was operating very near the surge condition, and for this reason the shift of the engine operating line due to variation in cooling-air-flow ratio could be serious; while the axial-flow compressor operated far from the compressor surge line, and for this reason the operating-line shift with cooling-air bleed is not a serious consideration.

The map of the turbine for the axial-flow-compressor engine, which is presented in figure 7(b), shows engine operating lines for cooling-air-flow ratios of 0, 0.02, 0.04, and 0.06. The operating lines cover the relative corrected engine speeds of 0.88 and 1.00 rated speed. The introduction of cooling air to the turbine had effects similar to those that were observed with the turbine of the centrifugal-flow engine. The increase to a cooling-air-flow ratio of 0.06 in the turbine caused a shift in the engine operating point and resulted in a decrease in corrected turbine specific work of 6 percent, a decrease in turbine efficiency of 2 points, and a decrease in turbine pressure ratio of 5 percent.

Whether there is an increase or decrease in compressor and turbine efficiency as the operation point changes due to bleeding the compressor for cooling air depends on how well the original matching of the two components was done at a design point that did not consider air-cooling. In designing a cooled-turbine engine, the matching should be done so that the compressor and turbine operate at their most efficient conditions when the design cooling-air flow is bled from the compressor. For this reason, better component efficiency can probably be obtained by considering cooling in the aerodynamic design of the engine rather than by altering an existing engine to permit cooling.

3021

Engine Performance Characteristics

Centrifugal-flow-compressor engine at rated speed. - The performance at rated speed of the engine with the centrifugal-flow compressor is presented in figure 8 as the variation of corrected specific thrust and corrected thrust specific fuel consumption with engine temperature ratio over a range of cooling-air-flow ratios and jet nozzle areas. The region between the limiting operating conditions of turbine limiting loading and compressor surge are considered. When a constant jet nozzle area (e.g., 1.80 sq ft) is considered, the engine temperature ratio increases at a rate of approximately 0.11 for each 0.01 increase in cooling-air-flow ratio. This increase in temperature ratio results in increases in corrected specific thrust and corrected thrust specific fuel consumption of 2.3 and 1.98 percent, respectively, for each 0.01 increase in cooling-air-flow ratio. The increase in thrust specific fuel consumption with increasing cooling-air-flow ratio at constant jet nozzle area is primarily due to the cooling losses. These losses are reflected in the specific turbine work, which is increased because of the additional work required by the cooling air and the decrease in turbine mass flow due to bleeding. The shape of the constant cooling-air-flow-ratio lines in figure 8(b) also should be noted. The reason for little or no change in thrust specific fuel consumption with increasing turbine-inlet temperature is that the turbine efficiency increases approximately 4 points at 0, 0.02, and 0.04 cooling-air-flow ratio, and approximately 3 points at 0.06 cooling-air-flow ratio over the temperature-ratio range considered, and the compressor pressure ratio and the compressor efficiency for this engine remain essentially constant. The relatively high level of the thrust specific fuel consumption of this engine is due to the low compressor efficiency (0.70) and compressor pressure ratio (4.0).

2-CJ

For high turbine-inlet temperatures or for noncritical turbine stator blades, it will be necessary to cool the turbine stator blades as well as the rotor blades. It was assumed herein that the cooling air for the stator blades would also be bled from the compressor discharge and exhausted into the main gas stream downstream of the turbine. A calculation was made for a total cooling-air-flow ratio of 0.06, of which 0.04 passed through the rotor blades and 0.02 passed through the stator blades at a constant jet nozzle area of 1.7 square feet. This condition of operation is also shown in figure 8. As would be expected, the point fell

between the 0.04 and 0.06 cooling-air-flow-ratio lines and near the jet-nozzle-area line for 1.7 square feet. The principal difference between this condition and that for 0.06 cooling-air-flow ratio for the rotor blades alone was that the 0.02 cooling-air-flow ratio for the stator blades does not require additional work from the turbine as does the rotor blade cooling air as it flows through the turbine rotor to the blade tip.

Also shown on figure 8 are the engine operating lines for rotor blade safety factors of 2.0 and 3.0 when a specific air-cooled blade was used in the turbine rotor. The noncritical blade material considered was Timken 17-22A(S). The blade was assumed to have the same cooling effectiveness as that described in reference 5 for configuration B, profile 1 (see fig. 2(a)), and the same aerodynamic performance as a standard turbine blade. For the case of a rotor blade safety factor of 3.0, which is considered conservative, the engine could operate over a range of turbine-inlet temperature from 2020° to 2310° R by varying the jet nozzle area. These temperatures are reached with a maximum cooling-air-flow ratio of approximately 0.02. The lower limit of inlet temperature is set by the condition of turbine limiting loading, and the upper limit approaches the condition of compressor surge. This range of turbine-inlet temperature permits an increase in specific thrust from approximately 52.0 to 63.4 pound-seconds per pound. This increase in thrust, due to the increase in turbine-inlet temperature and a slight decrease in turbine pressure ratio, is accompanied by an increase in thrust specific fuel consumption from 1.235 to 1.270.

A comparison was made of the engine with and without cooling. It was assumed that the design point of the uncooled engine was at a jet nozzle area of 1.80 square feet, an engine temperature ratio of approximately 3.85, and that this condition of turbine-inlet temperature limited the value of corrected specific thrust to 51.4 pound-seconds per pound. By using air-cooled turbine rotor blades, the limiting value of turbine-inlet temperature (inasmuch as it effects the turbine rotor blades) can be increased. With the air-cooled-blade operating line for a safety factor of 3.0 (see fig. 8(a)), a maximum value of turbine-inlet temperature of approximately 2310° R can be obtained. This maximum value is limited for this particular engine by the condition of compressor surge, not by blade temperature. At this value of turbine-inlet temperature, the specific thrust increased to 63.4 or approximately 23.5 percent over that of the uncooled engine at its limiting value of turbine-inlet temperature.

The thrust specific fuel consumption increases from 1.215 for the design point of the uncooled engine to 1.275 for the case of the air-cooled turbine rotor blades with a safety factor of 3.0 at the condition of compressor surge, an increase of approximately 4.9 percent (fig. 8(b)).

Centrifugal-flow-compressor engine at 87 percent of rated speed. - The performance of the centrifugal-compressor engine at 87 percent of rated speed (a condition slightly below cruise) was evaluated, and the operating lines of a cooled turbine blade operating at safety factors of 2.0 and 3.0 were calculated to determine whether or not cooling would be required when a noncritical turbine-blade material is used at this engine speed. These results are presented in figure 9. The type of plot presented for this engine speed is the same as that for the rated-speed calculations. The same trends of specific thrust and specific fuel consumption at constant jet nozzle area were obtained as at the rated-engine-speed condition. The cooled-turbine-blade operating lines for safety factors of 2.0 and 3.0 are not drawn on this figure, because the turbine-inlet temperatures and centrifugal blade stresses were low enough to permit operation at this speed without cooling air for all conditions covered on this map when stress-rupture data for 100-hour life are used. Thus the air-cooled-blade operating lines will be those for the zero cooling-air-flow ratio.

Axial-flow-compressor engine at rated speed. - Plots of the performance of the axial-flow-compressor engine for a range of jet nozzle areas and cooling-air-flow ratios are presented in figure 10. The results cover a range of cooling-air-flow ratios of 0 to 0.06. The minimum engine temperature ratio is limited by the conditions of turbine limiting loading, and the maximum by an assumed turbine-inlet temperature of 3000° R. If a constant jet nozzle area of 2.1 square feet is chosen, the increase in both the specific thrust and the thrust specific fuel consumption for this area can be evaluated. When the cooling-air-flow ratio is increased from 0 to 0.06, the engine temperature ratio increases from 3.74 to 4.42, or approximately 0.11 for every 0.01 increase in cooling-air-flow ratio. This increase in engine temperature ratio results in increased corrected specific thrust and corrected thrust specific fuel consumption of 2.5 percent and 2.27 percent, respectively, for every 0.01 increase in cooling-air-flow ratio. The increase in specific thrust was due to the increased turbine-inlet temperature, which, in turn, resulted in an increased thrust specific fuel consumption. The thrust specific fuel consumption was further increased by the decrease in turbine efficiency of approximately $1\frac{1}{2}$ points as the cooling-air-flow ratio increased from 0 to 0.06.

The point of engine operation when 6 percent of the compressor air is bled for cooling and when this air is divided between the turbine stator and rotor so that 4 percent passes through the rotor blades and 2 percent through the stators is also shown in figure 10 for a jet nozzle area of 2.2 square feet. Here, as was also the case for the centrifugal-compressor engine, the operating point fell very close to the jet-nozzle-area line of 2.2 square feet and midway between the 0.04 and 0.06 cooling-air-flow-ratio lines.

The operating lines for an air-cooled turbine blade of a noncritical material (Timken 17-22A(S)) operating with safety factors of 2.0 and 3.0 are shown on figure 10. This blade had the same cooling effectiveness as the one designated in reference 5 as profile 2, configuration H (see fig. 2(b)). As is shown in figure 10(a), this blade with a safety factor of 3.0 can operate from an engine temperature ratio of 3.64 at the turbine limiting-loading line to a temperature ratio of 4.84 at a cooling-air-flow ratio of 0.06. If it is assumed that the uncooled-engine design turbine-inlet temperature is limited to 1970° R ($T_3'/T_1' = 3.8$) because of the turbine rotor blades, the turbine-inlet temperature can be increased to 2510° R with air-cooled noncritical blades at 0.06 cooling-air-flow ratio. This increase in turbine-inlet temperature results in an increase in the specific thrust from approximately 55.0 to 69.0 pound-seconds per pound, or an increase of approximately 25.0 percent in the specific thrust compared with the design point of the uncooled engine. The increase in the specific fuel consumption that results from this increase in thrust and turbine-inlet temperature is shown by the blade operating lines in figure 10(b). If the line of safety factor equal to 3.0 is considered here, the specific fuel consumption increased from 1.019 for the uncooled condition to 1.196 pounds per hour per pound for a cooling-air-flow ratio of 0.06, an increase of about 17.4 percent.

The reason for the large difference in percentage increase in thrust specific fuel consumption for the centrifugal-flow and the axial-flow engines as the turbine-inlet temperatures are increased to the maximum amount permissible for the air-cooled blades considered can be determined by comparing figures 8(b) and 10(b). The air-cooled blade used in the centrifugal-flow machine requires much less cooling air than the blade used in the axial-flow machine, which results in smaller cooling losses for the centrifugal engine. For example, at an engine temperature ratio of 4.5, the air-cooled blade in the centrifugal-flow machine requires a cooling-air-flow ratio of about 0.02 at a safety factor of 3.0; and, at the same conditions, the blade in the axial-flow engine requires a cooling-air-flow ratio of approximately 0.04. This difference in required cooling-air-flow ratio is principally a result of the difference between the cooling effectivenesses of the two blades. The fact that the cooling-air-flow-ratio lines for the centrifugal-flow machine are relatively horizontal because of the increase in turbine efficiency also reduces the percentage increase in thrust specific fuel consumption. From the uncooled rated conditions to the cooled condition with a turbine-inlet temperature of 2310° R, the efficiency of the turbine in the centrifugal-flow engine increased approximately 3.8 points. The reverse was true of the turbine of the axial-flow engine, which suffered a decrease of 2 percent in turbine efficiency for the same relative conditions.

The comparatively low level of thrust specific fuel consumption for the axial-flow engine can be attributed to the higher compressor

efficiency (approx. 80 percent compared with 70 percent for the centrifugal-flow machine) and the higher compressor pressure ratio (approx. 5.5 compared with 4.0).

Axial-flow-compressor engine at 88 percent of rated speed. - The results for the cooled axial-flow engine are presented in figure 11 for 88 percent of rated speed. Here again, the trends of specific thrust, thrust specific fuel consumption, and turbine-inlet temperature ratio are the same as those obtained at the rated-speed condition. For the specific air-cooled blades considered, cooling is not needed at the cruise speed because of the lower centrifugal stresses and turbine-inlet temperatures.

Constant thrust operation. - Figure 12 shows the necessity of using turbine blades of high cooling effectiveness to minimize the cost of cooling in terms of thrust specific fuel consumption for the condition of constant specific thrust. Curves are presented in this figure for the centrifugal-compressor engine at constant engine speeds of 87 and 100 percent of rated speed and for corresponding values of constant specific thrust of 55.0 and 37.0 pound-seconds per pound. At rated engine speed, the specific fuel consumption increases from 1.217 at zero cooling-air-flow ratio to 1.361 pounds per hour per pound at 0.06 cooling-air-flow ratio, a rate of increase of approximately 1.96 percent for every 0.01 increase in cooling-air-flow ratio. At 87 percent of rated speed and a specific thrust of 37.0 pound-seconds per pound, the specific fuel consumption increases from 1.227 at zero cooling-air-flow ratio to 1.412 pounds per hour per pound at 0.06 cooling-air-flow ratio, a rate of increase of approximately 2.5 percent for every 0.01 increase in cooling-air-flow ratio. The operating points at a safety factor of 3.0 of the air-cooled turbine rotor blade considered herein for the centrifugal-flow engine are also shown in figure 12. At the cooling-air-flow ratio required for operation at a specific thrust of 55.0 pound-seconds per pound, the thrust specific fuel consumption is 1.24, an increase of approximately 2.0 percent over that required at zero cooling-air-flow ratio.

The effect of increasing cooling-air requirements on the thrust specific fuel consumption at a constant specific thrust for the axial-flow engine is presented in figure 13. This effect is shown for both rated-speed condition ($F/w_1\sqrt{\theta_1^*}$ = 55 lb-sec/lb) and the cruise speed ($F/w_1\sqrt{\theta_1^*}$ = 44.9 lb-sec/lb). The rate of increase of the corrected thrust specific fuel consumption with the cooling-air-flow ratio is approximately 2.08 percent for the rated-speed condition and 2.33 percent for the cruise-speed condition for every 0.01 increment in the cooling-air-flow ratio. The operation points of the air-cooled turbine rotor blade considered herein at a safety factor of 3.0 occurred at a corrected thrust specific fuel consumption of 1.044 at rated speed and 0.977 at the

cruise condition. At rated speed, this is an increase of 2.5 percent over that at zero cooling-air-flow ratio for a constant value of specific thrust. This increase is the cost of operating this particular blade configuration made of noncritical materials containing approximately 97-percent iron.

CONCLUSIONS

The effect of bleeding turbine rotor blade cooling air from the compressor discharge on the performance of contemporary turbojet engines was investigated. The two engines considered were a centrifugal-flow-compressor and an axial-flow-compressor engine. The performance for various cooling-air weight flows and jet nozzle areas was calculated with performance maps of the compressor and turbine for the particular engine being considered. The results summarized below are for the two specific engines discussed in this report and should not be generalized.

1. At rated engine conditions for a constant value of specific thrust, the thrust specific fuel consumption increased approximately 1.96 percent for the centrifugal-flow engine and 2.08 percent for the axial-flow engine for every 0.01 increase of cooling-air-flow ratio required.

2. At rated engine speed and a constant jet nozzle area, each increase of 0.01 in cooling-air-flow ratio resulted in an increase of 60° F in turbine-inlet temperature, an increase of 2.3 percent in specific thrust, and an increase of 1.98 percent in thrust specific fuel consumption for the centrifugal-flow-compressor engine. The effects on the axial-flow-compressor engine were similar to those for the centrifugal-flow-compressor engine, except that the increase in specific thrust was 2.5 percent and the increase in thrust specific fuel consumption was 2.27 percent for every 0.01 increase in cooling-air-flow ratio.

3. With the use of corrugated-insert air-cooled turbine rotor blades at a safety factor of 3.0, which is thought to be a conservative value, the turbine-inlet temperatures could be increased so that increases in specific thrust of approximately 24 percent for both engines could be realized. This increase in thrust was accompanied by an increase in specific fuel consumption of 4.9 percent for the centrifugal-flow engine and 17.4 percent for the axial-flow engine. The differences in the percentage increase in fuel consumption were due to the difference in cooling effectiveness of the two blades and an increase of approximately 4.0 points in turbine efficiency for the centrifugal-flow machine and a decrease of 2.0 points in turbine efficiency for the axial-flow engine.

4. At rated engine speed and a fixed jet nozzle area, bleeding 0.06 cooling-air-flow ratio from the centrifugal-flow compressor decreases the compressor weight flow by 2.0 percent, increases the compressor efficiency

by 1.0 point, and increases the turbine efficiency approximately 1 point. Bleeding the same amount from the axial-flow compressor increased the compressor pressure ratio 3.0 percent, increased the compressor efficiency 1/2 point, and decreased the turbine efficiency approximately 2.0 percent.

5. Since bleeding the compressor for turbine cooling air changes the compressor operating point in the direction of lower weight flow or higher compressor pressure ratio (depending upon the type of compressor being considered), cooling should be incorporated in the original engine design so that the highest possible component efficiencies can be realized and the danger of approaching the compressor surge region can be avoided.

The importance of the increase in thrust specific fuel consumption that accompanied the increases in specific thrust obtained with air-cooling cannot be effectively evaluated from an analysis of the engine alone. It is important that blades of high cooling effectiveness be utilized, but the final evaluation must give consideration to the aircraft and the type of mission to be accomplished. Factors such as range, flight time, portion of flight plan that requires turbine cooling, and possibility of elimination of afterburner have a large influence on how cooling will affect the over-all aircraft performance.

The use of an analysis such as presented in reference 9, which assumes constant component operating conditions, can possibly result in erroneous results at off-design operating conditions. This is evident from the effect of the variation of turbine efficiencies on the thrust specific fuel consumption for the two engines considered herein. It can be concluded that it is impossible to evaluate the trends of the effect on engine performance of using compressor bleed air for turbine cooling over a range of operating conditions unless a matching study based on the engine component characteristics and the blade cooling effectiveness is made.

Lewis Flight Propulsion Laboratory
National Advisory Committee for Aeronautics
Cleveland, Ohio, November 25, 1953

APPENDIX A

SYMBOLS

The following symbols are used in this report:

A	area, sq ft
F	thrust, lb
f	fuel-air ratio
g	standard gravitational acceleration, ft/sec^2
$\overline{H}$	lower heating value of fuel at 600° R, Btu/lb
h	enthalpy, Btu/lb
J	mechanical equivalent of heat, 778.2 ft-lb/Btu
K_1, K_2	constants
N	rotational speed, rpm
p	pressure, lb/sq ft
R	gas constant, ft-lb/($^\circ$F)(lb)
T	temperature, $^\circ$F or $^\circ$R
U	blade speed, ft/sec
V	velocity, ft/sec
w	weight flow, lb/sec
w_f	fuel weight flow, lb/hr
γ	ratio of specific heats
Δ	prefix indicating change or increment
δ	pressure-correction ratio, p'/p'_0

ϵ $\left[\left(\frac{\gamma+1}{2}\right)^{\frac{\gamma}{\gamma-1}}\frac{1}{\gamma}\right]_C \Big/ \left[\left(\frac{\gamma+1}{2}\right)^{\frac{\gamma}{\gamma-1}}\frac{1}{\gamma}\right]_H$

η efficiency

θ^* temperature-correction ratio, $\frac{\frac{2\gamma}{\gamma+1}gRT'}{\left(\frac{2\gamma}{\gamma+1}gRT'\right)_O}$

ξ $\left(\frac{\gamma_C+1}{\gamma_C-1}\right)\left(\frac{\gamma_H-1}{\gamma_H+1}\right)$

φ temperature-difference ratio, $\frac{\overline{T}_{g,e} - \overline{T}_B}{\overline{T}_{g,e} - \overline{T}_{a,e,h}}$

ψ_h $\frac{(h-h_O)(1+f)}{f}$, Btu/lb

Ω work, Btu/sec

Subscripts:

a rotor and blade cooling air

B blade

b burner

C cold

c compressor

cr critical

e effective

g gas

H hot

h hub or root of blade

ISB compressor interstage bleed

id	ideal
ov	compressor overboard bleed
R	relative; used to designate ratio of compressor and turbine parameters at any operating condition to those at design condition
T	turbine
t	tip
u	tangential
x	axial
0	NACA sea-level standard; dry air, zero fuel-air ratio when used with h
1 - 9	engine stations (see fig. 1)

Superscripts:

—	indicates average value
'	indicates total or stagnation conditions

APPENDIX B

CALCULATION PROCEDURE FOR COMPRESSOR AND TURBINE MATCHING AND ENGINE PERFORMANCE FOR VARIOUS COOLING-AIR-FLOW RATIOS

The engine stations used in the following calculations are shown in figure 1. The first step was to assume an operating point on the compressor map along a constant corrected compressor speed line. The compressor map is a plot of the compressor weight flow $w_1\sqrt{\theta_1^*}/\delta_1$ against the compressor total-pressure ratio p_2'/p_1'. Lines of constant corrected compressor speed $N/\sqrt{\theta_1^*}$ and constant compressor efficiency η_c are also included on the map. (All symbols are defined in appendix A.) When the compressor operating point had been chosen, the values of η_c, $w_1\sqrt{\theta_1^*}/\delta_1$, and p_2'/p_1' were fixed, and it was then possible to calculate the weight flow at engine stations 2, 3, and 4 with the following equations:

$$w_2 = w_1 - w_{ISB}, \text{ lb/sec} \tag{B1}$$

$$w_3 = (1 + f)(w_2 - w_{ov} - w_a), \text{ lb/sec} \tag{B2}$$

$$w_4 = w_5 = w_3 + w_a + w_{ISB}, \text{ lb/sec} \tag{B3}$$

The items w_{ov}, w_{ISB}, and w_a in terms of the engine calculation stations of figure 1 are

$$w_{ISB} = w_7 + w_8$$

$$w_{ov} = w_9$$

$$w_a = w_6$$

The terms w_{ov} and w_{ISB} were used herein only for the axial-flow-compressor engine.

Turbine work. - The work output of the turbine, defined as the work to drive the compressor plus the work to pump the cooling air from the point where it enters the turbine rotor to the blade tip, could also be determined at this point in the calculations. The specific work or total enthalpy drop across the turbine is

$$\Delta h_T' = \frac{\Omega_c + \Omega_a}{w_3}, \text{ Btu/lb} \tag{B4}$$

The work required to drive the compressor Ω_c is defined by

$$\Omega_c = w_2(h'_2 - h'_1) + w_{ISB}(h'_{ISB} - h'_1), \text{ Btu/sec} \quad (B5)$$

The total enthalpy rise across the compressor in equation (B5) was evaluated from

$$h'_2 - h'_1 = \frac{h'_{2,id} - h'_1}{\eta_c}, \text{ Btu/lb} \quad (B6)$$

where the ideal or isentropic total enthalpy at the compressor discharge was obtained by the method presented in reference 12 with the compressor pressure ratio as read from the compressor map. The total enthalpy at the point of interstage bleed h'_{ISB} was evaluated from temperature measurements in a standard engine test made on the axial-flow compressor used herein. Since the cooling air enters the turbine rotors considered herein at essentially the center line of the rotor, the work required to pump the cooling air from this point to the blade tip is

$$\Omega_a = \frac{w_a V^2_{a,u,t}}{gJ} \quad (B7)$$

Turbine-inlet temperature. - The total temperature at the turbine inlet was evaluated by an iteration process using an assumed value of $(w_3\sqrt{\theta^*_3}/\delta_3)_H$ and known values of w_3 and δ_3. The value of w_3 was determined in equation (B2), and the value of δ_3 was obtained from the relation

$$\delta_3 = \left(1 - \frac{p'_2 - p'_3}{p'_2}\right)\left(\frac{p'_2}{p'_1}\right)\left(\frac{p'_1}{p'_0}\right) \quad (B8)$$

where $(p'_2 - p'_3)/p'_2$ is the burner pressure-loss parameter.

For the turbines considered herein at the speeds investigated, the cold-air performance results indicated that the turbine stator blades were choked; and, therefore $w_3\sqrt{\theta^*_3}/\delta_3$ was constant. That is,

$$\left(\frac{w_3\sqrt{\theta^*_3}}{\delta_3}\right)_C = K_1 \quad (B9)$$

The corrected turbine-inlet weight flow at the cold condition was related to that of the hot engine by (see ref. 10)

$$\left(\frac{w_3\sqrt{\theta_3^*}}{A_3\delta_3}\right)_C \epsilon = \left(\frac{w_3\sqrt{\theta_3^*}}{A_3\delta_3}\right)_H \quad \text{(B10)}$$

By using an assumed $(w_3\sqrt{\theta_3^*}/\delta_3)_H$ and the known values of w_3 and δ_3, an approximate value of θ_3^* and hence T_3' could be determined. With this value of T_3', the value of ϵ evaluated for $\gamma_{3,C}$ of 1.40 and $(w_3\sqrt{\theta_3^*}/\delta_3)_H$ could be evaluated from equation (B10).

This procedure was repeated until a value of the turbine-inlet temperature was obtained that gave agreement between the assumed value of $(w_3\sqrt{\theta_3^*}/\delta_3)_H$ and the value obtained from equation (B10).

Jet nozzle area. - The jet nozzle area A_5 was evaluated from the following equation:

$$A_5 = \frac{\frac{w_5}{p_5}\sqrt{\frac{R(\gamma_5-1)T_5'}{2\gamma_5 g}}}{\left\{\left(\frac{p_5'}{p_5}\right)^{\frac{\gamma_5-1}{\gamma_5}}\left[\left(\frac{p_5'}{p_5}\right)^{\frac{\gamma_5-1}{\gamma_5}} - 1\right]\right\}^{\frac{1}{2}}}, \text{ sq ft} \quad \text{(B11)}$$

where

p_5 jet nozzle static pressure (atmospheric), lb/sq ft

p_5' jet nozzle total pressure (assumed equal to $p_{4,x}'$), lb/sq ft

The value of w_5 was obtained in equation (B3). The value of p_5'/p_5 was obtained from the following relation for pressure ratios below critical:

$$\frac{p_5'}{p_5} = \delta_3\left(\frac{p_{4,x}'}{p_3'}\right)_H \quad \text{(B12)}$$

When the ratio of the total pressure at the jet nozzle to atmospheric pressure was greater than critical, a critical pressure ratio of 1.851 (for the temperature range of 1500° to 1800° R) was used in equation (B11) to evaluate the jet nozzle area. In equation (B12), the turbine pressure ratio $(p_{4,x}'/p_3')_H$ was obtained from the cold-air turbine map and the following relation presented in reference 10:

$$\left\{\frac{\gamma+1}{\gamma-1}\left[1-\left(\frac{p'_{4,x}}{p'_3}\right)^{\frac{\gamma-1}{\gamma}}\right]\right\}_H = \left\{\frac{\gamma+1}{\gamma-1}\left[1-\left(\frac{p'_{4,x}}{p'_3}\right)^{\frac{\gamma-1}{\gamma}}\right]\right\}_C$$

When this equation was solved for $(p'_{4,x}/p'_3)_H$, the following equation resulted:

$$\left(\frac{p'_{4,x}}{p'_3}\right)_H = \left\{1-\xi\left[1-\left(\frac{p'_{4,x}}{p'_3}\right)_C^{\frac{\gamma_{3,C}-1}{\gamma_{3,C}}}\right]\right\}^{\gamma_{3,H}/(\gamma_{3,H}-1)} \qquad \text{(B13)}$$

where $\gamma_{3,C} = 1.40$, and $\gamma_{3,H}$ is based on T'_3 and $f = 0.0135$.

The total temperature at the jet nozzle T'_5 was determined from the total enthalpy at this station h'_5 and the charts presented in reference 12 for a fuel-air ratio of 0.0135. The total enthalpy at station 5 was evaluated from the following equation:

$$h'_5 = \frac{w_3 h'_4 + w_{ISB} h'_{ISB} + w_a\left(h'_2 + \frac{\overline{V}^2_{a,u,t}}{gJ}\right)}{w_5}, \text{ Btu/lb} \qquad \text{(B14)}$$

where

$$h'_4 = h'_3 - \Delta h'_T, \text{ Btu/lb} \qquad \text{(B15)}$$

and h'_3 was evaluated from T'_3 and reference 12 for $f = 0.0135$. [It should be noted (eq. (B14)) that the interstage bleed air is exhausted into the main combustion-gas stream downstream of the turbine.]

Engine specific thrust and specific fuel consumption. - The corrected specific thrust was defined as $F/w_1\sqrt{\theta_1}^*$. When the jet nozzle pressure ratio was less than critical, the engine thrust was calculated with the relation

$$F = w_5\left\{\frac{2\gamma_5 RT'_5}{g(\gamma_5-1)}\left[1-\left(\frac{p_5}{p'_5}\right)^{\frac{\gamma_5-1}{\gamma_5}}\right]\right\}^{\frac{1}{2}}, \text{ lb} \qquad \text{(B16)}$$

where γ_5 was evaluated from T_5', $f = 0.0135$, $p_5 = p_0$, $p_5' = p_{4,x}'$, and w_5 was evaluated in equation (B3).

When the jet nozzle pressure ratio was supercritical, equation (B16) was modified to

$$F = w_5 \left\{ \frac{2\gamma_5 R T_5'}{g(\gamma_5 - 1)} \left[1 - \left(\frac{p_5}{p_5'} \right)_{cr}^{\frac{\gamma_5 - 1}{\gamma_5}} \right] \right\}^{\frac{1}{2}} + (p_5 - p_0)A_5, \text{ lb} \qquad \text{(B17)}$$

where $p_5 = p_5'(p_5/p_5')_{cr}$, and $(p_5/p_5')_{cr}$ was assumed equal to 0.540 for the range of T_5' from 1500° to 1800° R.

The corrected thrust specific fuel consumption was defined as $w_f/F\sqrt{\theta_1^*}$. The fuel weight-flow rate w_f was evaluated from (see ref. 12)

$$w_f = \frac{h_{0,3} - h_{0,2}}{\eta_b \overline{H} - h_{0,3} - \psi_h} \times (w_2 - w_{ov} - w_a) \times 3600, \text{ lb/hr} \qquad \text{(B18)}$$

A lower heating value $\overline{H}$ of 18,605 Btu per pound was used for the fuel. The enthalpy of the fuel was neglected. The fuel consumption calculated from equation (B18) was based on the actual fuel-air ratio required for the turbine-inlet temperature that was obtained from equation (B10).

REFERENCES

1. Esgar, Jack B., and Clure, John L.: Experimental Investigation of Air-Cooled Turbine Blades in Turbojet Engine. X - Endurance Evaluation of Several Tube-Filled Rotor Blades. NACA RM E52B13, 1952.

2. Cochran, Reeves R., Stepka, Francis S., and Krasner, Morton H.: Experimental Investigation of Air-Cooled Turbine Blades in Turbojet Engine. XI - Internal-Strut-Supported Rotor Blade. NACA RM E52C21, 1952.

3. Bartoo, Edward R., and Clure, John L.: Experimental Investigation of Air-Cooled Turbine Blades in Turbojet Engine. XII - Cooling Effectiveness of a Blade with an Insert and with Fins made of a Continuous Corrugated Sheet. NACA RM E52F24, 1952.

4. Bartoo, Edward R., and Clure, John L.: Experimental Investigation of Air-Cooled Turbine Blades in Turbojet Engine. XIII - Endurance Evaluation of Several Protective Coatings Applied to Turbine Blades of Nonstrategic Steels. NACA RM E53E18, 1953.

5. Ziemer, Robert R., and Slone, Henry O.: Analytical Procedures for Rapid Selection of Coolant Passage Configurations for Air-Cooled Turbine Rotor Blades and for Evaluation of Heat-Transfer, Strength, and Pressure-Loss Characteristics. NACA RM E52G18, 1952.

6. Schramm, Wilson B., and Ziemer, Robert R.: Investigations of Air-Cooled Turbine Rotors for Turbojet Engines. I - Experimental Disk Temperature Distribution in Modified J33 Split-Disk Rotor at Speeds up to 6000 RPM. NACA RM E51I11, 1952.

7. Nachtigall, Alfred J., Zalabak, Charles F., and Ziemer, Robert R.: Investigations of Air-Cooled Turbine Rotors for Turbojet Engines. III - Experimental Cooling-Air Impeller Performance and Turbine Rotor Temperatures in Modified J33 Split-Disk Rotor up to Speeds of 10,000 RPM. NACA RM E52C12, 1952.

8. Moseson, Merland L., Krasner, Morton H., and Ziemer, Robert R.: Mechanical Design Analysis of Several Noncritical Air-Cooled Turbine Disks and a Corrugated-Insert Air-Cooled Turbine Rotor Blade. NACA RM E53E21, 1953.

9. Schramm, Wilson B., Nachtigall, Alfred J., and Arne, Vernon L.: Preliminary Analysis of Effects of Air Cooling Turbine Blades on Turbojet-Engine Performance. NACA RM E50E22, 1950.

10. Heaton, Thomas R., Slivka, William R., and Westra, Leonard F.: Cold-Air Investigation of a Turbine with Nontwisted Rotor Blades Suitable for Air Cooling. NACA RM E52A25, 1952.

11. Goldstein, Arthur W.: Analysis of Performance of a Jet Engine from Characteristics of Components. I - Aerodynamic and Matching Characteristics of Turbine Component Determined with Cold Air. NACA Rep. 878, 1947. (Supersedes NACA TN 1459.)

12. English, Robert E., and Wachtl, William W.: Charts of Thermodynamic Properties of Air and Combustion Products from 300° to 3500° R. NACA TN 2071, 1950.

3021

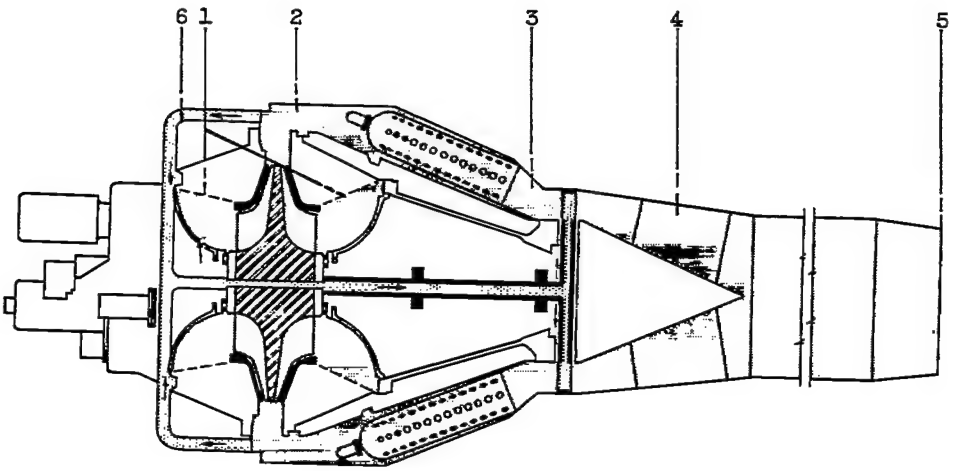

(a) Turbojet engine with centrifugal compressor.

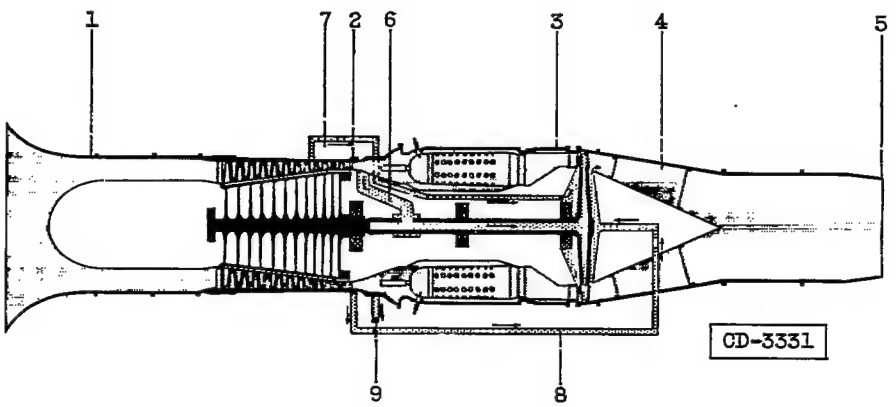

(b) Turbojet engine with axial-flow compressor.

Station	Description
1	Compressor inlet (sea-level static)
2	Compressor outlet
3	Turbine inlet
4	Turbine outlet
5	Jet nozzle
6	Compressor-outlet bleed for blade cooling air
7	Compressor eighth-stage bleed (cooling air for forward face of turbine)
8	Compressor-outlet bleed (cooling air for rear face of turbine)
9	Compressor overboard bleed

Figure 1. - Calculation stations for turbojet engines with air-cooled turbines.

(a) Turbine blade for centrifugal-compressor engine.

(b) Turbine blade for axial-flow-compressor engine.

Figure 2. - Enlarged cross-sectional views of air-cooled corrugated-insert turbine rotor blades.

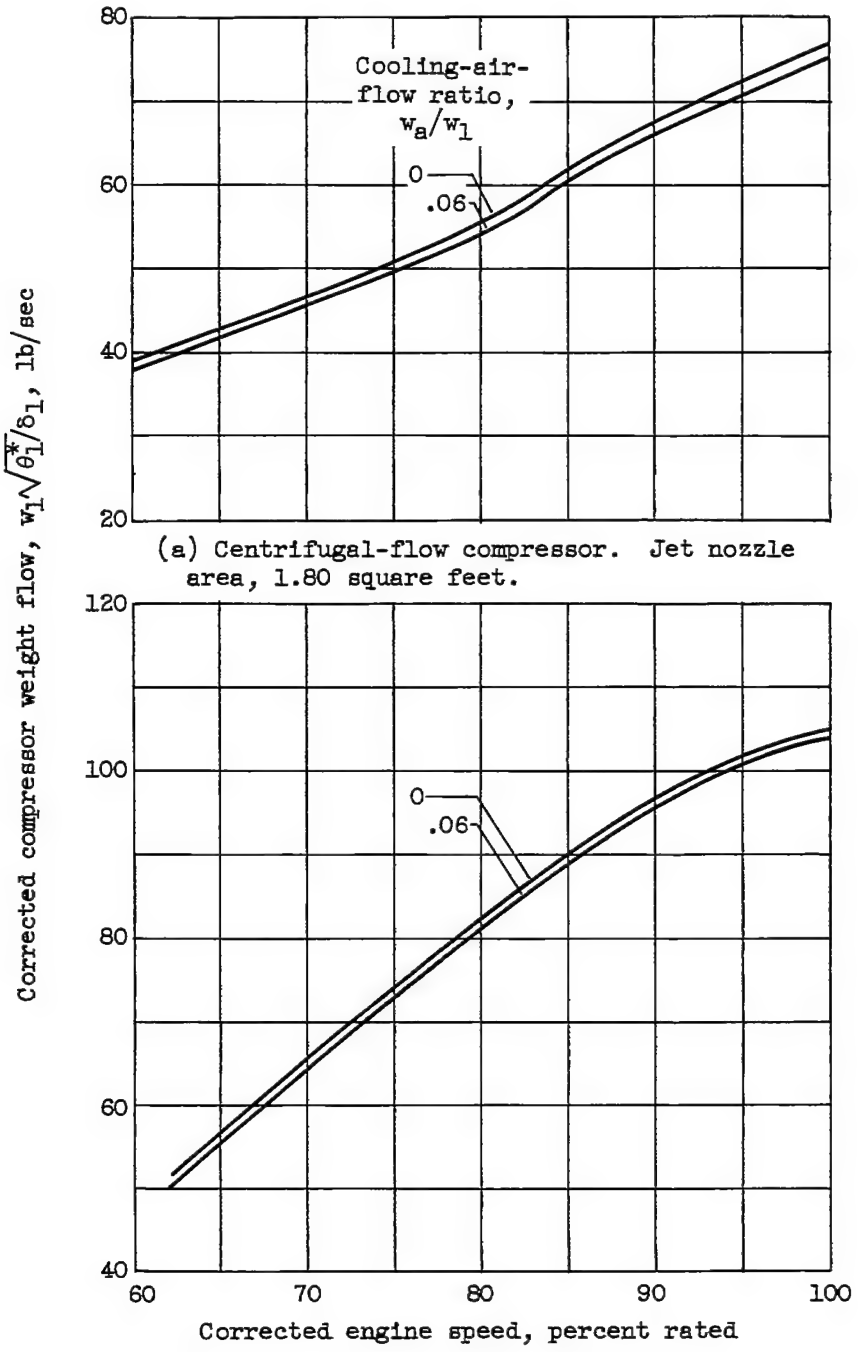

(a) Centrifugal-flow compressor. Jet nozzle area, 1.80 square feet.

(b) Axial-flow compressor. Jet nozzle area, 2.06 square feet.

Figure 3. - Effect of cooling-air bleed on compressor weight flow over range of engine speeds.

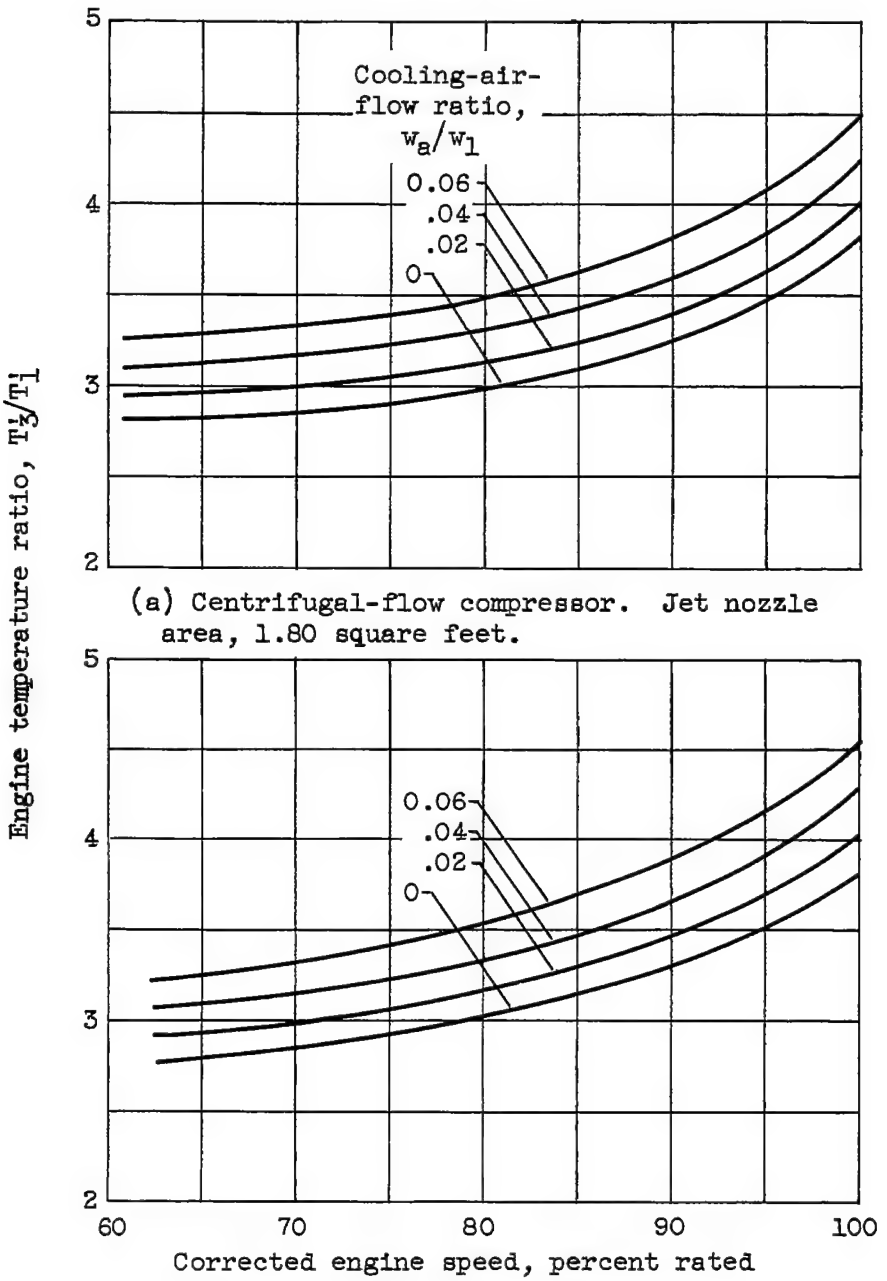

(a) Centrifugal-flow compressor. Jet nozzle area, 1.80 square feet.

(b) Axial-flow compressor. Jet nozzle area, 2.06 square feet.

Figure 4. - Variation of engine temperature ratio with percent of rated corrected engine speed over range of cooling-air-flow ratios with fixed jet nozzle area.

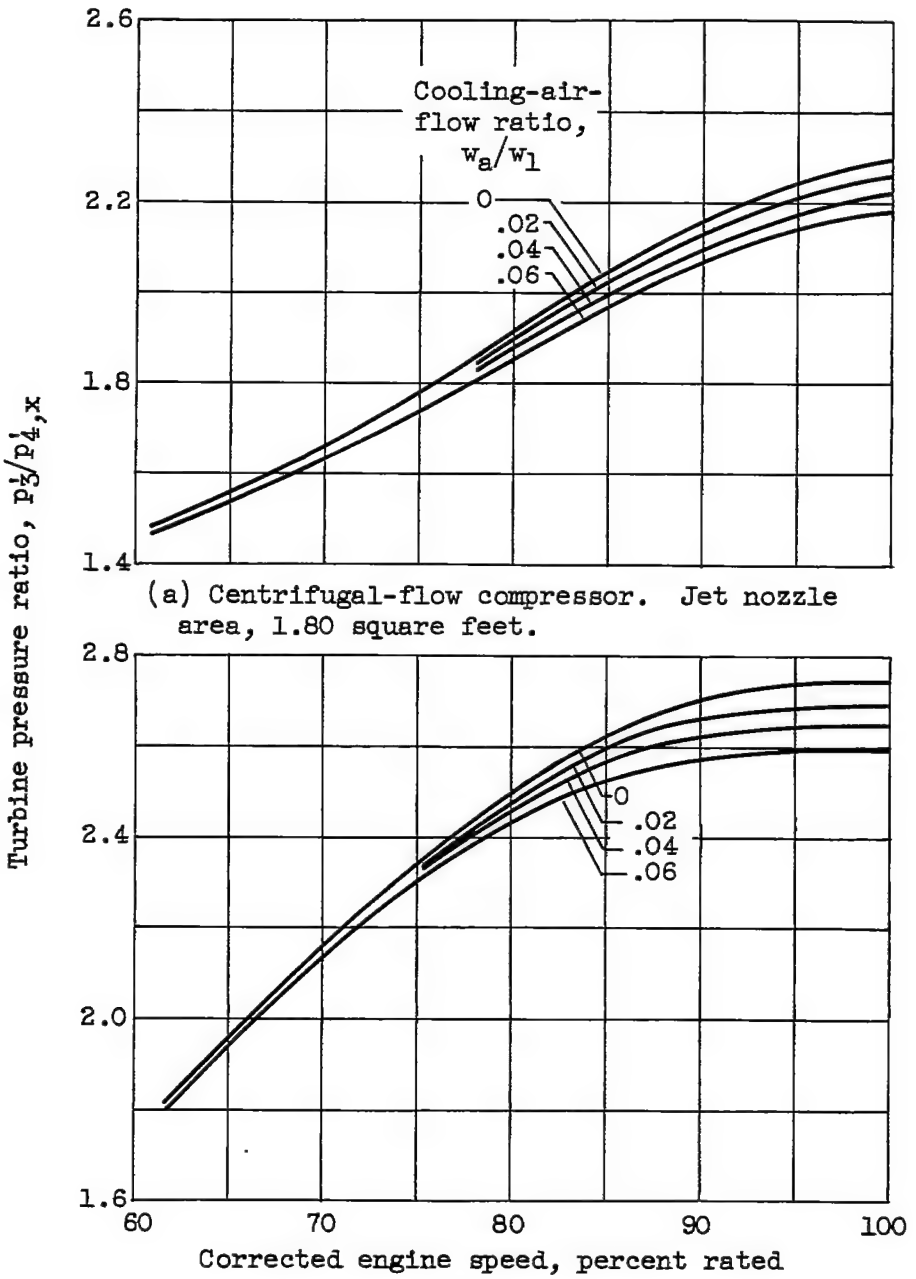

(a) Centrifugal-flow compressor. Jet nozzle area, 1.80 square feet.

(b) Axial-flow compressor. Jet nozzle area, 2.06 square feet.

Figure 5. - Variation of turbine pressure ratio with percent of rated corrected engine speed over range of cooling-air-flow ratios with fixed jet nozzle area.

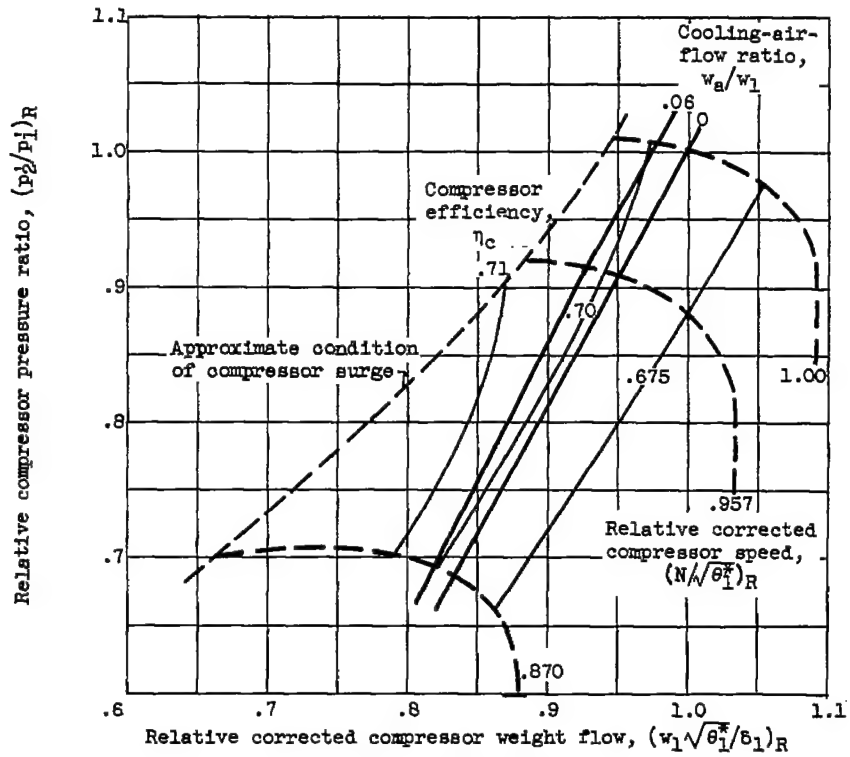

(a) Compressor map.

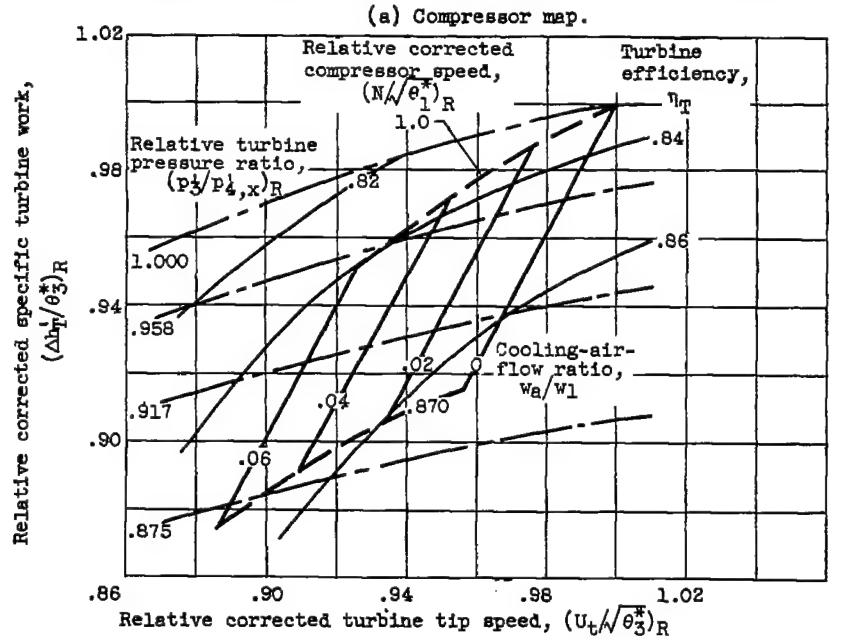

(b) Turbine map.

Figure 6. - Centrifugal-flow-engine operating lines on relative performance maps for several cooling-air-flow ratios. Jet nozzle area, 1.80 square feet.

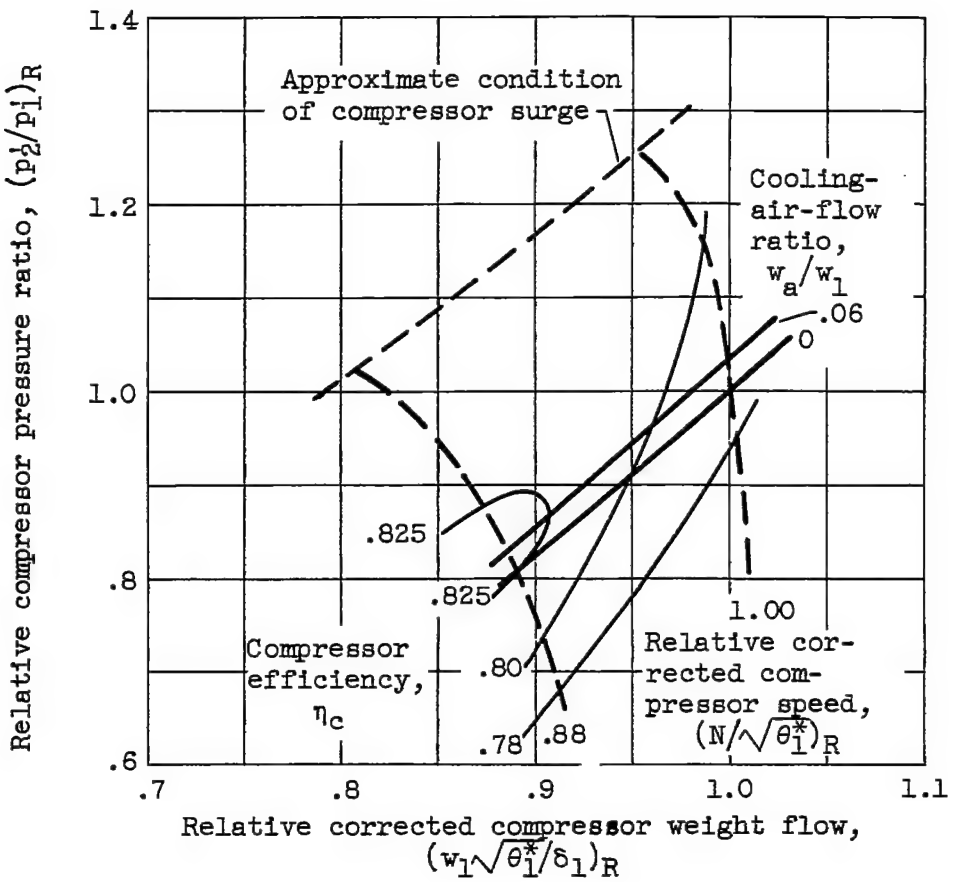

(a) Compressor map.

Figure 7. - Axial-flow-engine operating lines on relative performance maps for several cooling-air-flow ratios. Jet nozzle area, 2.06 square feet.

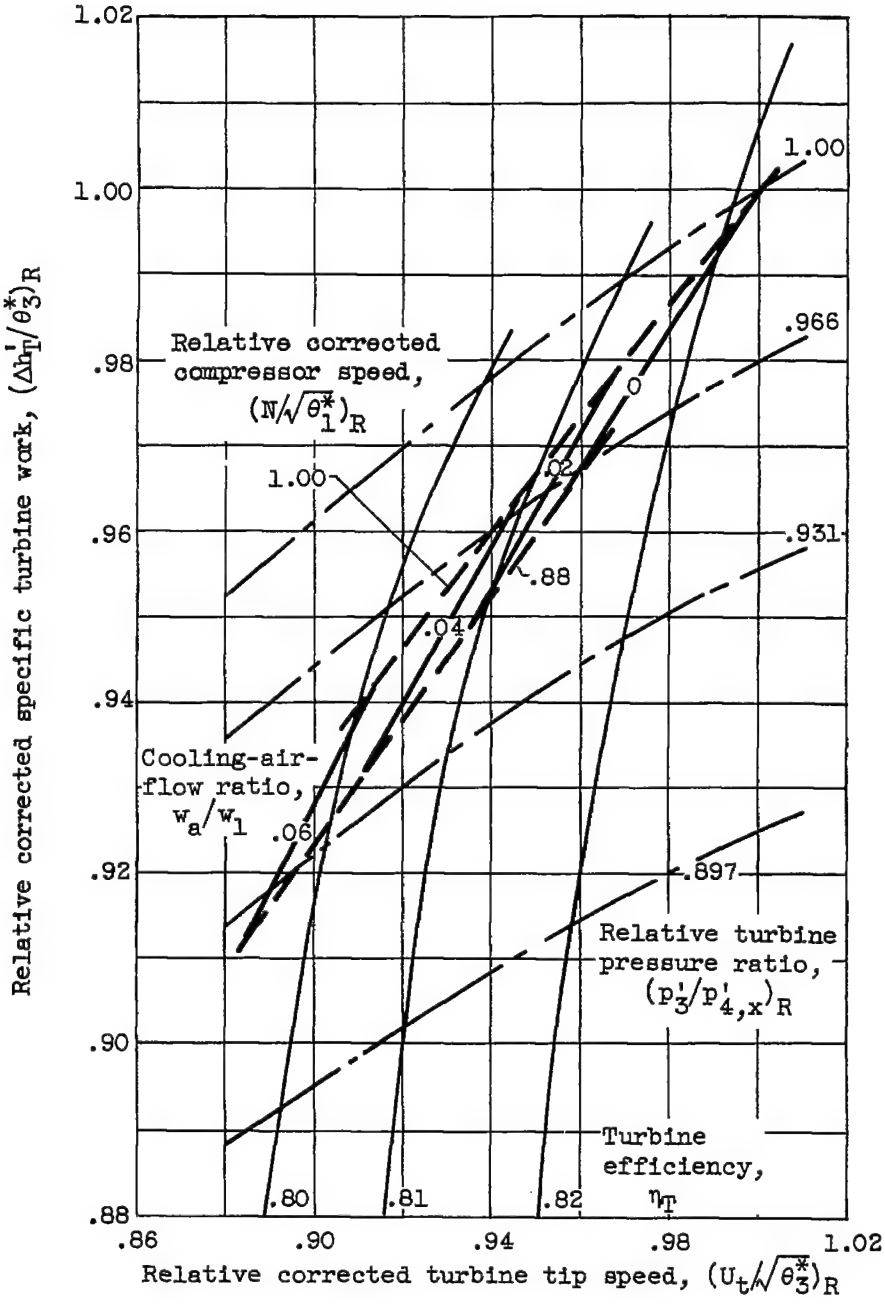

(b) Turbine map.

Figure 7. - Concluded. Axial-flow-engine operating lines on relative performance maps for several cooling-air-flow ratios. Jet nozzle area, 2.06 square feet.

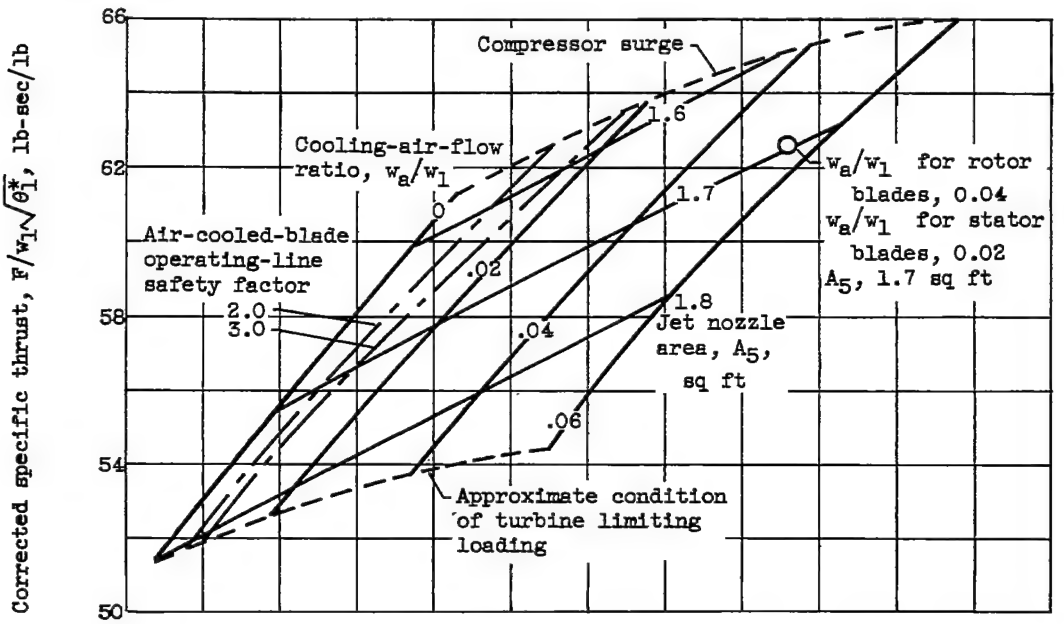

(a) Variation of corrected specific thrust with engine temperature ratio for four cooling-air-flow ratios over range of jet nozzle areas.

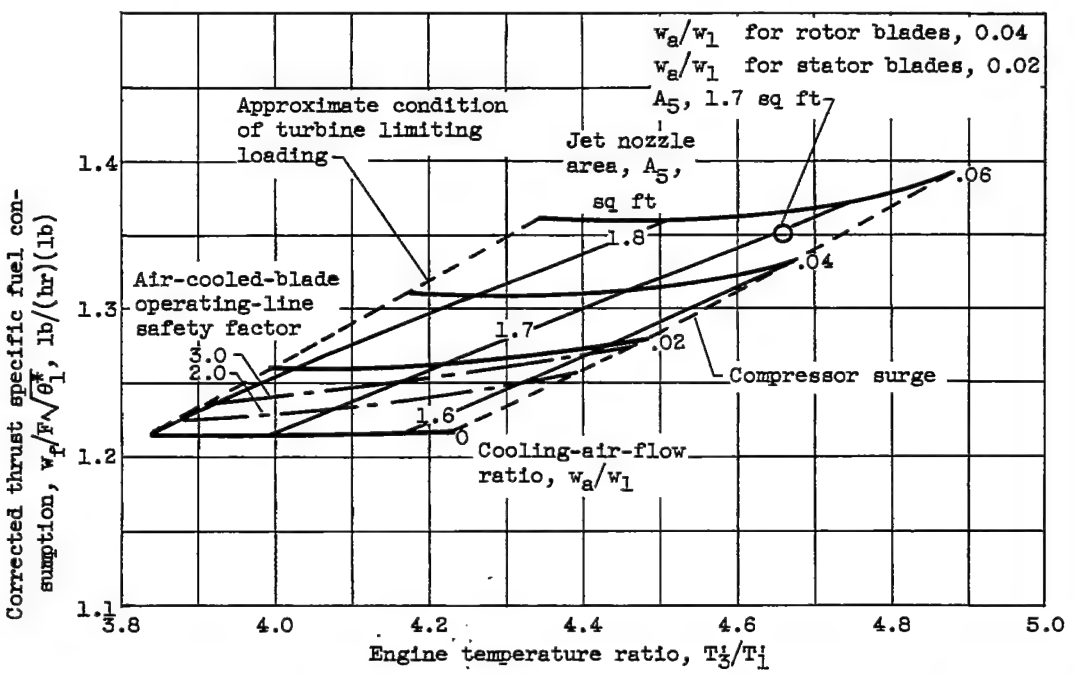

(b) Variation of corrected thrust specific fuel consumption with engine temperature ratio for four cooling-air-flow ratios over range of jet nozzle areas.

Figure 8. - Typical centrifugal-flow-compressor turbojet-engine performance at rated speed.

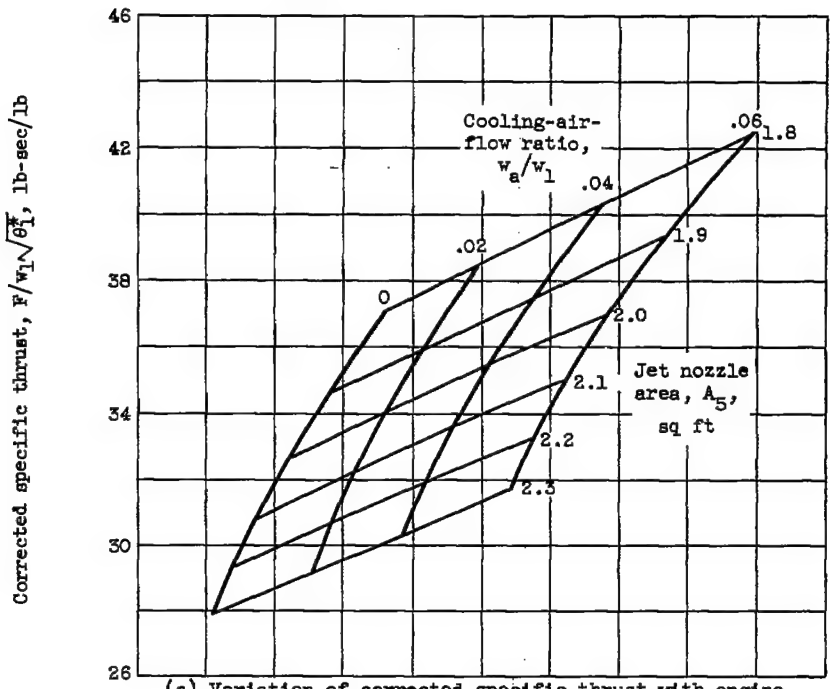

(a) Variation of corrected specific thrust with engine temperature ratio for four cooling-air-flow ratios over range of jet nozzle areas.

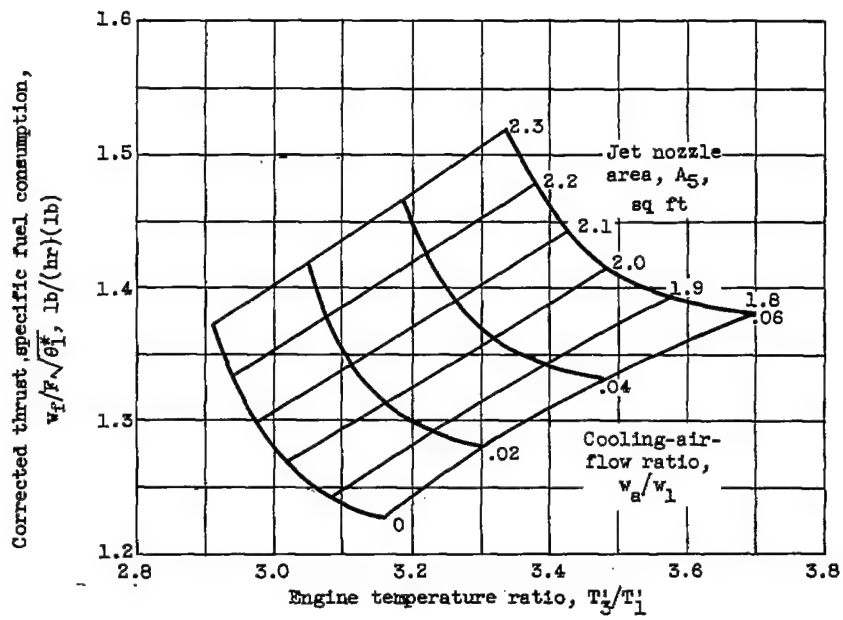

(b) Variation of corrected thrust specific fuel consumption with engine temperature ratio for four cooling-air-flow ratios over range of jet nozzle areas.

Figure 9. - Typical centrifugal-flow-compressor turbojet-engine performance at 87 percent of rated speed.

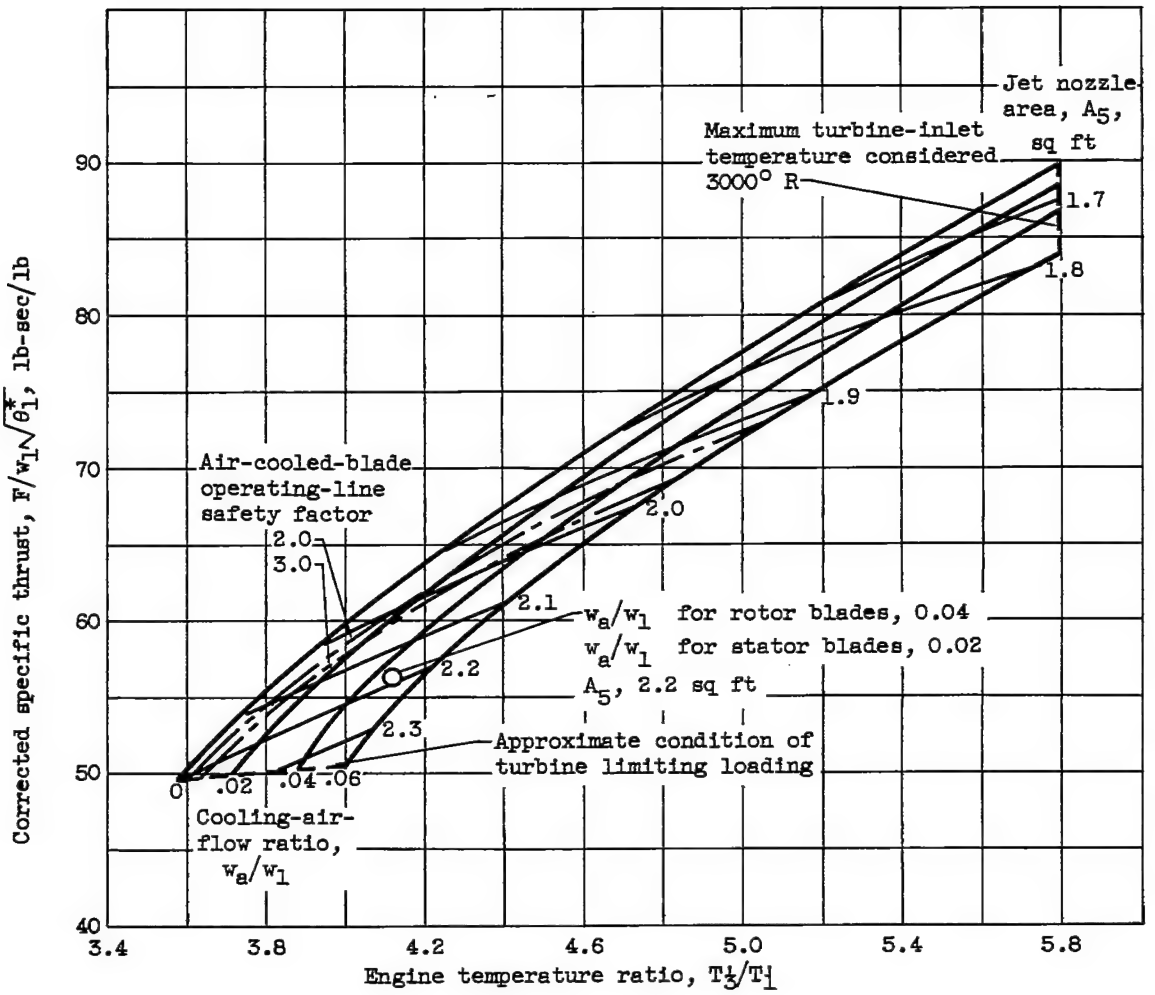

(a) Variation of corrected specific thrust with engine temperature ratio for four cooling-air-flow ratios over range of jet nozzle areas.

Figure 10. - Typical axial-flow-compressor turbojet-engine performance at rated speed.

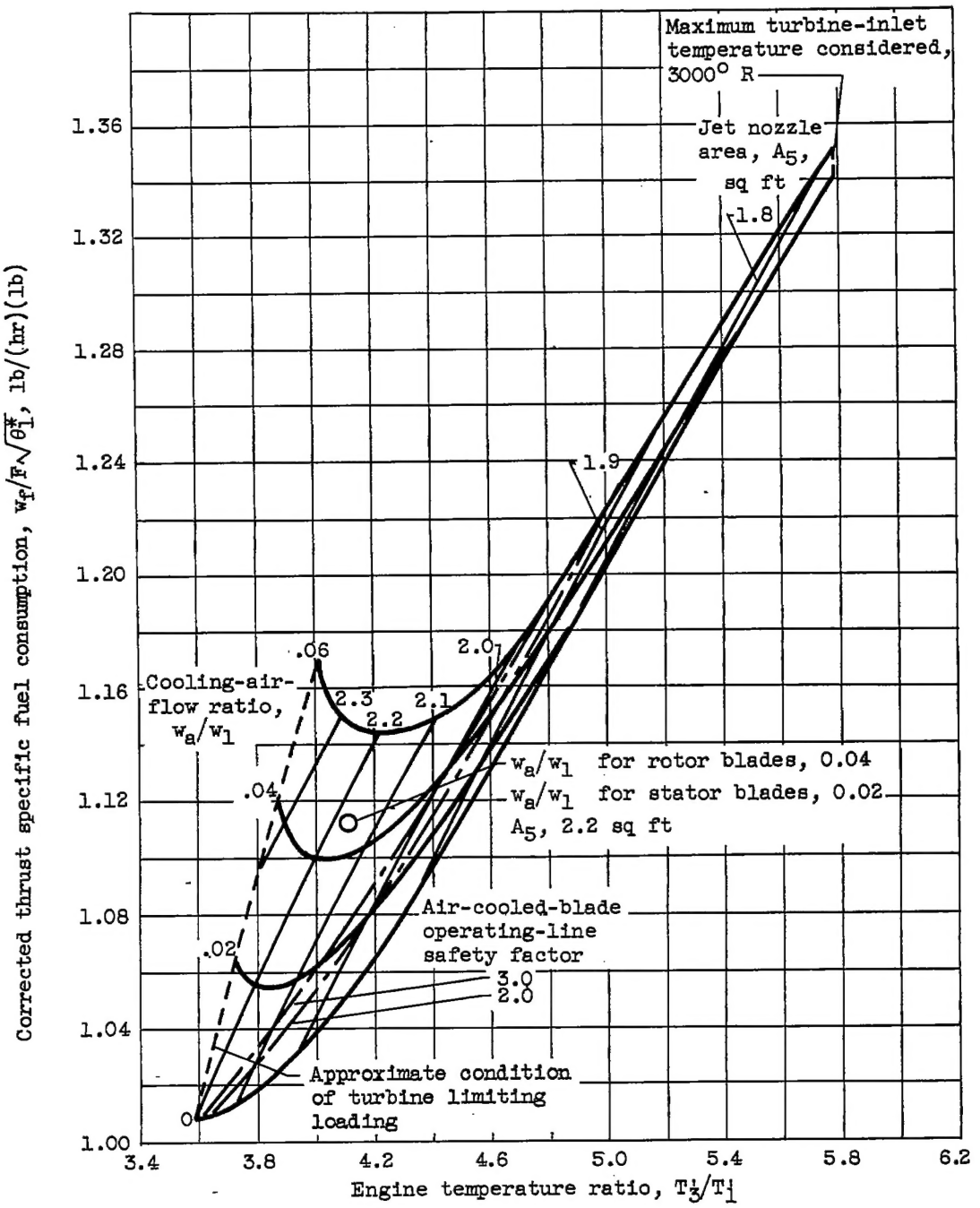

(b) Variation of corrected thrust specific fuel consumption with engine temperature ratio for four cooling-air-flow ratios over range of jet nozzle areas.

Figure 10. - Concluded. Typical axial-flow-compressor turbojet-engine performance at rated speed.

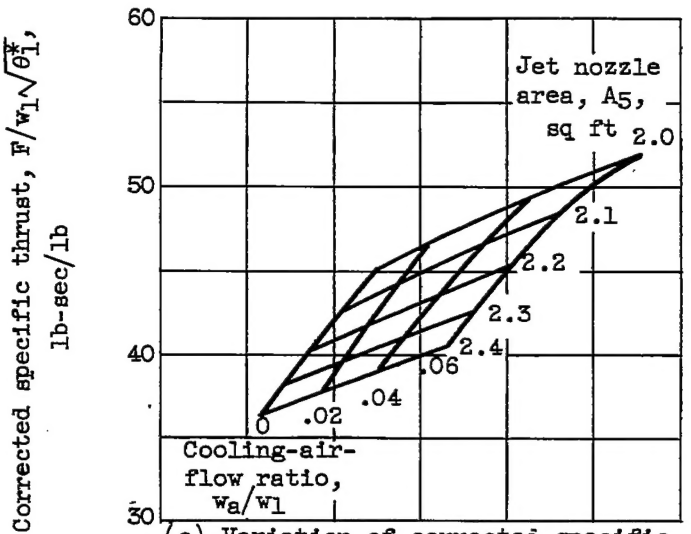

(a) Variation of corrected specific thrust with engine temperature ratio for four cooling-air-flow ratios over range of jet nozzle areas.

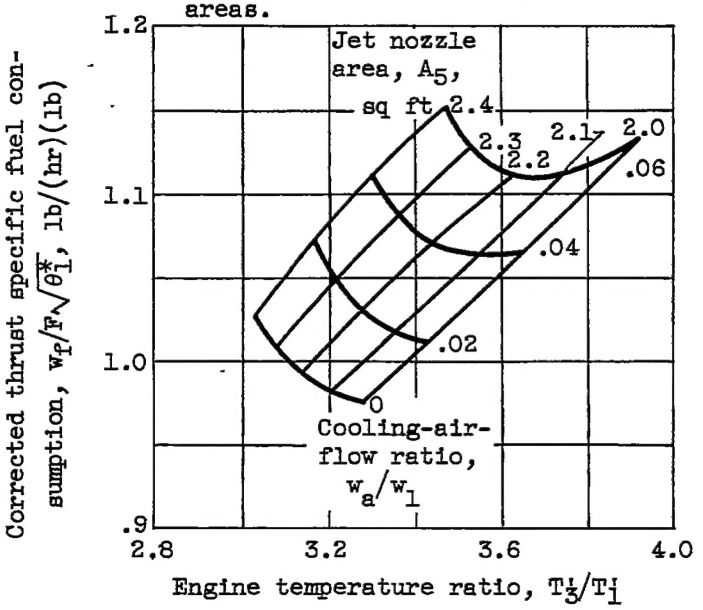

(b) Variation of corrected thrust specific fuel consumption with engine temperature ratio for four cooling-air-flow ratios over range of jet nozzle areas.

Figure 11. - Typical axial-flow-compressor turbojet-engine performance at 88 percent of rated speed.

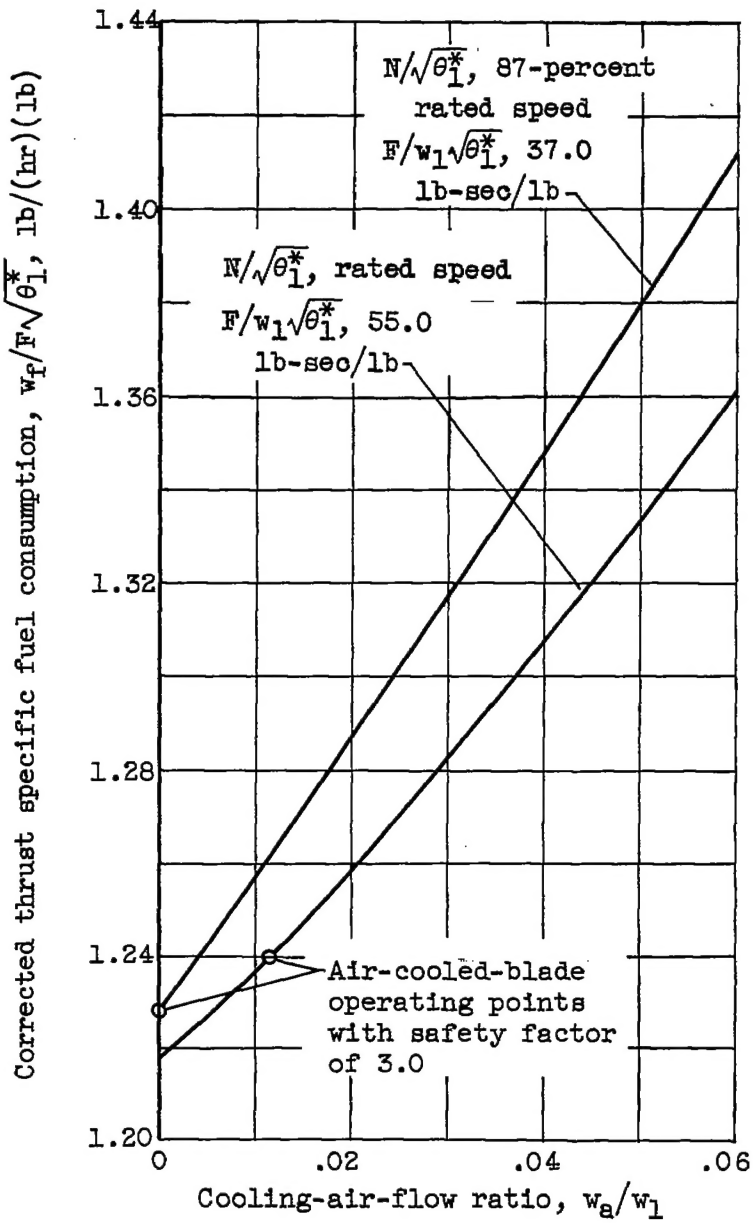

Figure 12. - Variation of thrust specific fuel consumption with cooling-air-flow ratio for constant values of corrected specific thrust at two corrected engine speeds. Centrifugal-flow compressor.

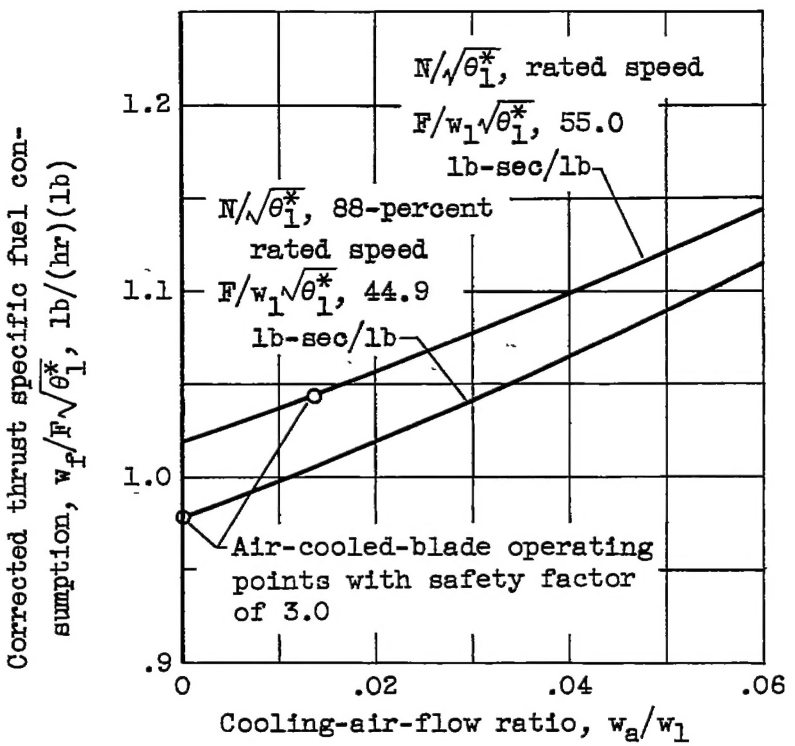

Figure 13. - Variation of thrust specific fuel consumption with cooling-air-flow ratio for constant values of corrected specific thrust at two corrected engine speeds. Axial-flow compressor.